

Generation of Structured Light and Controlled-NOT Gate in Microwave Regime

Parkhi Bhardwaj* and Shubhrangshu Dasgupta

Department of Physics, Indian Institute of Technology Ropar, Rupnagar, Punjab 140001, India

(Dated: October 25, 2024)

We propose how to generate beams with non-zero orbital angular momentum in the microwave domain using atomic vapor medium and coherent control techniques. Our approach utilizes a difference frequency generation process in a centrosymmetric medium in the presence of a dc electric field for frequency conversion and parametric amplification. By employing phase matching conditions and orbital angular momentum conservation, we constructed a Controlled NOT gate using a three-level atomic configuration. By generating Laguerre-Gaussian fields in the microwave domain, we open up novel possibilities for advanced information processing in wireless communication and potential applications in quantum technologies.

I. INTRODUCTION

Electromagnetic (EM) waves possess energy and both linear and angular momenta. The spin angular momentum (SAM) is associated with the circularly polarized light while the orbital angular momentum (OAM) is related to the spatial phase structure of light. Allen *et al.* discovered that light beams with an azimuthal phase dependence of $\exp(il\phi)$ carry an OAM of $l\hbar$ per photon, where ϕ is the azimuthal coordinate in the cross-section of the beam, and l can take any positive or negative integer value [1, 2]. The wavefront of the beam becomes helical in shape, with l number of twists in one wavelength, while the Gaussian intensity profile displays a vortex (or null) at the center in the transverse direction of propagation. Such light beams can be generated by various methods, e.g., cylindrical lens pairs [3], computer-generated holograms [4], spatial light modulators [5], liquid crystal spatial light modulators [6], etc. A detailed review of these techniques can be found in [7].

In the last few years, researchers have been primarily interested in the interaction between atoms and light which have OAM. The OAM of a field can be transferred to another field via light-matter interaction using certain protocols that depend upon the energy level configuration of the atoms [8–14]. It was shown in a V-type atomic configuration that by introducing coherence between the excited states (i.e., in an electric dipole-forbidden transition) using a microwave field, it is possible to transfer the OAM from a field with Laguerre-Gaussian (LG) intensity profile to a plane wave [15]. A similar effect can be obtained in a four-level ladder-type configuration [16]. The coherence in the excited states in a V-type configuration can also be induced via vacuum-induced coherence [17], instead of a microwave field, and this can, as well, lead to the transfer of the OAM from an LG beam to a weak planar field [15]. The authors in [18] have extended their result of a Λ -type configuration to a generalized tripod system to show that an initial vortex state can be transformed into many, by preparing the atom in a superposition of the ground states. In a symmetry-broken ladder-type three-level quantum system, OAM transfer can be more efficiently done, via three-wave mixing, in Autler-Townes splitting regime rather than in the

electromagnetically induced transparency regime [19].

Until now, most of the research has focused on generating LG beams in the optical domain. However, due to the rapid advancement of wireless communication technology and an increasing demand for broadband data transfer, data centers, and cloud-based services [20], there is a pressing need to enhance spectral efficiency and system capacity, in the microwave regime and beyond. To address this challenge, fields in the microwave regime with OAM pose as a promising candidate for information transfer. The OAM offers additional degrees of freedom to simultaneously carry information at the same frequency within a single communication channel [21], that too without increasing the frequency bandwidth [22]. Consequently, the utilization of OAM in wireless communications has become an area of intense research, especially in the microwave regime [23], necessitating developing techniques for generating waves with microwave frequencies along with the OAM.

Microwave radiation cannot be generated via natural atomic transitions alone and so, we must manipulate the atomic energy levels. In this context, we use the Stark effect [24] and second-order nonlinear processes [25–27] in atomic vapors to generate microwave radiation. Even-order nonlinear processes are typically prohibited in centrosymmetric media under the dipole approximation. However, they can become significant if electric quadrupole and magnetic dipole matrix elements are included [28], though these effects are generally weak and difficult to measure. Second-order nonlinearity can be observed in atomic vapor subjected to an electric or magnetic field, which breaks the symmetry by mixing states of even and odd parity [24, 29]. Here, we propose a novel method for generating an LG beam in the microwave regime. Our model relies on three-wave mixing, which becomes feasible in an atomic quantum system excited by collinear lasers in the presence of a DC electric field. We carefully calibrate the electric field intensity to ensure an energy splitting that surpasses the fine structure splitting, setting it at approximately $10^3 - 10^4$ V/cm [24]. This setup enables a cyclic energy level configuration to transfer the OAM from the input field to the output field.

In this paper, we demonstrate, for the first time, the generation of a field in the microwave regime using optical fields and discuss the efficiency of this process. Subsequently, we introduce phase singularity on the generated field through the coupling and control fields, individually selecting them as LG

* parkhi.21phz0013@iitrpr.ac.in

beams. We then explore how the intensity of the generated field can be reshaped by manipulating the strength of the control field. Finally, we successfully generate the hollow Gaussian beam (HGB) by incorporating the Gaussian profile of the control field. Then we discuss the construction of a controlled NOT (CNOT) gate in the OAM basis using three-level atomic energy level configuration.

The structure of the paper is as follows. In Sec. II, we show how a V-type configuration can lead to microwave generation. The study of a Λ configuration in the same context is described in Sec. III. How a CNOT gate can be created in these configurations is discussed in Sec. IV. In Sec. V, we propose ways of creating dipole-allowed transitions to facilitate microwave generation. We conclude the paper in Sec. VI.

II. MICROWAVE GENERATION WITH V-TYPE CONFIGURATION

We consider a V-type energy level configuration of the atomic system as illustrated in Fig. 1a. The symmetry of the system can be disrupted by applying a dc electric field in the z -direction, resulting in the mixing of energy levels of even and odd parity. The frequency gap between the energy levels can be adjusted by the applied dc electric field.

To generate a microwave field, we apply a dc electric field on the atom that splits the energy levels, mixes the energy levels of even and odd parity, and creates a gap in the order of the microwave frequency domain between the energy levels of the same principle quantum number, according to the strength of the electric field. The transitions to the excited states $|2\rangle$ and $|3\rangle$ from the ground state $|1\rangle$ are induced by two electromagnetic fields with amplitudes \vec{E}_1 and \vec{E}_2 and frequencies ω_1 and ω_2 , respectively. The transitions $|1\rangle \leftrightarrow |3\rangle$, $|3\rangle \leftrightarrow |2\rangle$, and $|1\rangle \leftrightarrow |2\rangle$ are electric dipole-allowed, with respective electric dipole moments $\vec{\mu}_{31}$, $\vec{\mu}_{32}$ and $\vec{\mu}_{21}$. The Rabi frequencies of the applied fields are defined as $\Omega_1 = \frac{\vec{\mu}_{31} \cdot \vec{E}_1}{\hbar}$ and $\Omega_2 = \frac{\vec{\mu}_{21} \cdot \vec{E}_2}{\hbar}$. This energy level configuration can be observed in hydrogen-like alkali atoms in the presence of a dc electric field. This quantum system exhibits second-order nonlinear wave-mixing because of the lack of inversion symmetry, leading to the generation of a new frequency $\omega_3 = \omega_1 - \omega_2$, via difference frequency generation. This requires the following phase matching condition: $\vec{k}_3 = \vec{k}_1 - \vec{k}_2$. The three-wave phase matching condition allows for coupling between the two excited states, with the transition occurring in the microwave frequency regime.

We assume that one of these electromagnetic fields in the visible regime possesses the LG intensity profile, along with a non-zero OAM. The respective Rabi frequencies for both the fields are given by (in cylindrical coordinates)

$$\Omega_j(r, \phi) = \Omega_{0j} \frac{1}{\sqrt{|l_j|!}} \left(\frac{\sqrt{2}r}{w} \right)^{|l_j|} e^{-r^2/w^2} e^{il_j\phi}, \quad j = 1, 2, \quad (1)$$

where Ω_{0j} , l_j and w define the constant Rabi frequency, the topological charge of the j th field, and beam waist respectively.

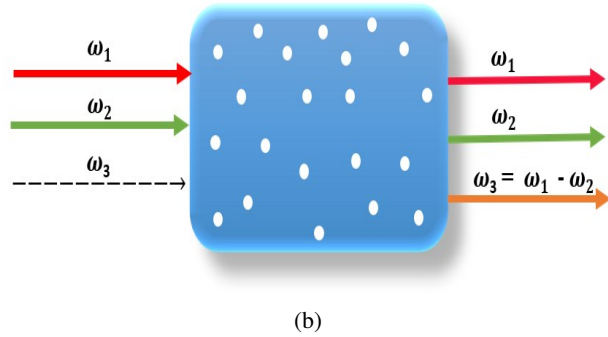
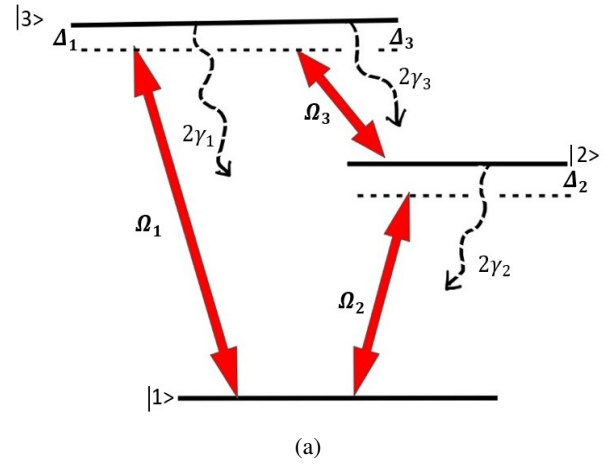


FIG. 1: (a) Relevant energy level configuration of the V-type three-level atomic system. (b) A schematic to depict the three wave mixing in atomic vapor

The interaction between the atom and the EM fields is described by the following Hamiltonian, under electric-dipole and rotating wave approximations (RWA):

$$H = \hbar\omega_{21} |2\rangle \langle 2| + \hbar\omega_{31} |3\rangle \langle 3| - (\hbar\Omega_1 e^{-i\omega_1 t} |1\rangle \langle 3| + \hbar\Omega_2 e^{-i\omega_2 t} |1\rangle \langle 2| + \hbar\Omega_3 e^{-i\omega_3 t} |2\rangle \langle 3| + h.c.), \quad (2)$$

where Ω_3 is the Rabi frequency of the generated signal field. In order to find the dynamical behavior of the atomic population and coherences of the V-type system, we use the Liouville equation:

$$\dot{\rho} = -\frac{i}{\hbar} [H, \rho] + L\rho, \quad (3)$$

where the second term describes the spontaneous decay processes of the atomic system. Then using the Liouville equation, the density matrix equations under the RWA are given

by

$$\begin{aligned}
\dot{\tilde{\rho}}_{22} &= i\Omega_2^* \tilde{\rho}_{12} - i\Omega_2 \tilde{\rho}_{21} + i\Omega_3 \tilde{\rho}_{32} - i\Omega_3^* \tilde{\rho}_{23} \\
&\quad - 2\gamma_{12} \tilde{\rho}_{22} + 2\gamma_{32} \tilde{\rho}_{33} \\
\dot{\tilde{\rho}}_{33} &= i\Omega_1^* \tilde{\rho}_{13} - i\Omega_1 \tilde{\rho}_{31} - i\Omega_3 \tilde{\rho}_{32} + i\Omega_3^* \tilde{\rho}_{23} \\
&\quad - 2(\gamma_{13} + \gamma_{32}) \tilde{\rho}_{33} \\
\dot{\tilde{\rho}}_{12} &= -i\Omega_2 (\tilde{\rho}_{22} - \tilde{\rho}_{11}) + i\Omega_1 \tilde{\rho}_{32} - i\Omega_3^* \tilde{\rho}_{13} \\
&\quad + (i\Delta_2 - \gamma_{12}) \tilde{\rho}_{12} \\
\dot{\tilde{\rho}}_{13} &= -i\Omega_1 (\tilde{\rho}_{33} - \tilde{\rho}_{11}) + i\Omega_2 \tilde{\rho}_{23} - i\Omega_3 \tilde{\rho}_{12} \\
&\quad + (i\Delta_1 - (\gamma_{13} + \gamma_{32})) \tilde{\rho}_{13} \\
\dot{\tilde{\rho}}_{23} &= -i\Omega_1 \tilde{\rho}_{21} + i\Omega_2^* \tilde{\rho}_{13} + i\Omega_3 (\tilde{\rho}_{22} - \tilde{\rho}_{33}) \\
&\quad + (i\Delta_3 - (\gamma_{13} + \gamma_{12} + \gamma_{32})) \tilde{\rho}_{23}.
\end{aligned} \tag{4}$$

where $\Delta_1 = \omega_1 - \omega_{13}$, $\Delta_2 = \omega_2 - \omega_{12}$, and $\Delta_3 = \omega_3 - \omega_{32}$ are the detunings of fields. We assume that E_1 is the control field and E_2 is the coupling field. The above density matrix obeys the conditions $\sum_i \rho_{ii} = 1$ and $\tilde{\rho}_{ij} = \tilde{\rho}_{ji}^*$. To obtain the above equations we have used the following transformations:

$$\rho_{13} = \tilde{\rho}_{13} e^{-i\omega_1 t}, \rho_{12} = \tilde{\rho}_{12} e^{-i\omega_2 t}, \rho_{23} = \tilde{\rho}_{23} e^{-i\omega_3 t}. \tag{5}$$

In Eq. (4), γ_{13} , γ_{12} , and γ_{32} are the spontaneous decay rates of the states $|1\rangle$, $|2\rangle$ and $|3\rangle$ respectively.

In the weak-field limit, we can expand the density matrix elements up to first order in Ω_2 : $\tilde{\rho}_{ij} = \tilde{\rho}_{ij}^{(0)} + \Omega_2 \tilde{\rho}_{ij}^{(1)} + \dots$, where $\tilde{\rho}_{ij}^{(k)}$ are the k th order approximations. We assume that detunings Δ_1 , Δ_2 , and Δ_3 are all zero, and the decay rates γ_{12} and γ_{13} are equal to γ , while γ_{32} is equal to 2γ . This allows us to obtain the following expressions for the first order of $\tilde{\rho}_{32}$ and $\tilde{\rho}_{21}$ in the steady state:

$$\tilde{\rho}_{32}^{(1)} = \frac{-6\Omega_1 \Omega_2^*}{18\gamma^2 + |\Omega_1|^2}, \quad \tilde{\rho}_{21}^{(1)} = \frac{-18i\gamma \Omega_2^* + 6\Omega_1 \Omega_3}{18\gamma^2 + |\Omega_1|^2}. \tag{6}$$

Here the real part of coherence $\tilde{\rho}_{32}^{(1)}$ carries information about the beam profile, which is then transferred to the microwave field through interaction between light and matter. On the other hand, the imaginary part of the coherence $\tilde{\rho}_{32}$ corresponds to the amplification or absorption of the generated microwave field. If the imaginary part of coherence is negative (positive), it corresponds to the gain or amplification (absorption).

We next study the beam propagation of the microwave field, generated through the atomic coherence $\tilde{\rho}_{32}$. For a time-independent microwave field propagating in the z direction, the Maxwell's equation can be written in the slowly varying envelope approximation as

$$\frac{\partial \Omega_3}{\partial z} = i \frac{\alpha_{32} \gamma_{32}}{2L} \tilde{\rho}_{32}^{(1)}, \quad \frac{\partial \Omega_2}{\partial z} = i \frac{\alpha_{21} \gamma_{21}}{2L} \tilde{\rho}_{21}^{(1)}, \tag{7}$$

where $\alpha_{32} = \alpha_{21} = \alpha$ is the optical depth and L is the length of the medium. Substituting the Eq. (6) into Eq. (7) with initial condition $\Omega_3(z=0) = 0$ and $\Omega_2(z=0) = \Omega_2(0)$. We get the following expression for the Rabi frequency of the microwave

field:

$$\Omega_3(z) = \frac{-4i\Omega_2^*(0)\Omega_1}{\sqrt{(9\gamma + 8|\Omega_1|^2)}} \exp\left(\frac{9\alpha\gamma^2 z}{2L(18\gamma^2 + |\Omega_1|^2)}\right) \sinh\left(\frac{3\alpha\gamma z \sqrt{9\gamma^2 + 8|\Omega_1|^2}}{2(18\gamma^2 + |\Omega_1|^2)L}\right). \tag{8}$$

A. Efficiency of Three-wave mixing

To evaluate the efficiency of the above process of a third field through three-wave mixing, we define a dimensionless quantity $\eta = (|\Omega_3(z)|/|\Omega_2(0)|)^2$ [30], given by

$$\eta = \frac{16\Omega_1}{(9\gamma + 8|\Omega_1|^2)} \exp\left(\frac{9\alpha\gamma^2 z}{L(18\gamma^2 + |\Omega_1|^2)}\right) \sinh^2\left(\frac{3\alpha\gamma z \sqrt{9\gamma^2 + 8|\Omega_1|^2}}{2(18\gamma^2 + |\Omega_1|^2)L}\right). \tag{9}$$

We plot in Fig. 2a, η as a function of the parameter Z/L , where, $Z = z\alpha$ is the modified propagation distance, for various strengths of the field Ω_1 . As shown in this figure, the efficiency of three-wave mixing begins to increase with increasing Z/L . Since nonlinear processes are based on momentum and energy conservation [31], the strong control field Ω_1 leads to the amplification of the coupling field Ω_2 and the generated signal field Ω_3 . Since the medium in consideration exhibits second-order nonlinearity, the interaction of Ω_1 and Ω_2 generates a signal field that gets amplified as it keeps propagating further into the medium. After traveling a certain distance into the medium, a generated field emerges with its amplitude, dependent on the strength of the control field. This process involves frequency conversion with gain, referring to the parametric amplification of the generated field. The efficiency factor η exhibits exponential growth with respect to the Z . Therefore, the gain of the generated field depends upon both the optical depth α and the strength of the control field Ω_1 . While it may be challenging to dynamically control the atomic number density of the medium (and hence, α), we can monitor Ω_1 to achieve the desired outcome. We show in Fig. 2b the variation of the efficiency η with $(|\Omega_1|/\gamma)^2$. It is clear from this figure that there is an optimal value of Ω_1 , for which the η is maximum.

B. Transfer of OAM from the coupling field to the generated field

Next we consider transferring the OAM of a coupling field to the generated field. From the Eq. 8, we can see that the Ω_3 is proportional to $\Omega_2^*(0)$. This means that a field of topological charge, l_2 can be formed if the coupling field contains a charge $-l_2$ at $z = 0$. We show in the Table I, the intensity and phase profile of Ω_3 and the imaginary part of ρ_{32} at a propagation distance $Z = L$ for $l_2 = 1, 2$, and 3. As we increase the value of l_2 , the area of the null point of intensity also increases and the phase changes accordingly: for $l_2 = 1$ it changes from 0

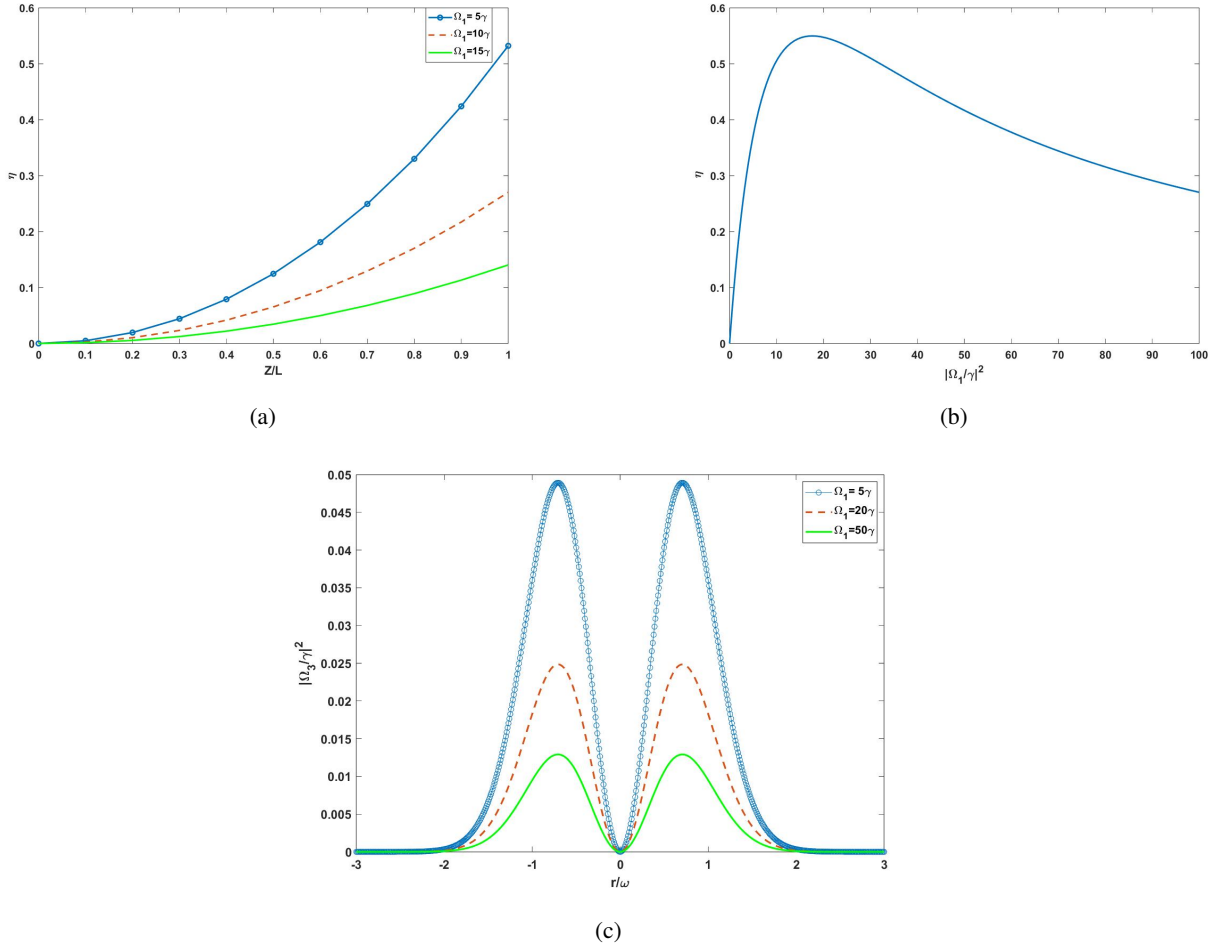


FIG. 2: Variation of (a) η as a function of Z/L for $\Omega_1 = 5\gamma$ (blue (solid-o)), $\Omega_1 = 10\gamma$ (red (dash)), and $\Omega_1 = 15\gamma$ (green (solid)), (b) η as a function of $|\Omega_1/\gamma|^2$, and (c) $(|\Omega_3|/\gamma)^2$ with respect to r/ω for $\Omega_1 = 5\gamma$ (blue (solid-o)), $\Omega_1 = 20\gamma$ (red (dash)), and $\Omega_1 = 50\gamma$ (green (solid)). We have chosen $\Omega_2 = 0.5\gamma$, $l_2 = 1$, and $Z = L$.

to 2π ; for $l_2 = 2$, from 0 to 4π , and for $l_2 = 3$, from 0 to 6π . If l_2 is the topological charge of the generated field, one can see $2l_2$ numbers of petals in the third column of Table I, in which the positive (negative) values of $\text{imag}(\rho_{32})$ corresponds to the absorption (gain) of the generated field. We also show in Fig.2c the radial distribution of the intensity of the generated field with topological charge $l_2 = 1$ for $\Omega_1 = 5\gamma$, 10γ , and 15γ . We find that for larger Ω_1 , the intensity of the generated field gets reduced.

C. Transfer of OAM from the Control Field to the Generated Field

So far, we treated the coupling field as an LG field. Since the generated field Ω_3 is also proportional to Ω_1 [see Eq. 8], the phase singularity of the control field Ω_1 can also be transferred to the generated field. Now, we are considering the control field to be the LG field. To understand the intensity pattern, we show in Fig. 3a the variation of η with respect

to r/w , for different values of Ω_{01} . This plot illustrates that one ring of the generated LG field with $l_3 = 1$ starts to split into two rings around the area of null intensity as we increase the strength of the control field. In Fig. 3b, we display the intensity profile of the generated field for different values of Ω_{01} . We see appearances of two concentric rings of intensity (resembling two doughnuts), for larger Ω_{01} .

D. Generation of Hollow Gaussian Beam

As we have seen in the preceding subsections, just by monitoring the strength of the control field, one can shape the generated light and split a single doughnut into two, which form an LG beam with azimuthal mode l_3 . If the intensity profile of the control field is Gaussian ($l_1=0$), the lower values of Ω_{01} yield a Gaussian intensity pattern for generated field. However, as we progressively increase Ω_{01} , the generated beam splits into ring, forming a hollow Gaussian beam. We show in Fig.4a the normalized intensity of the generated field for dif-

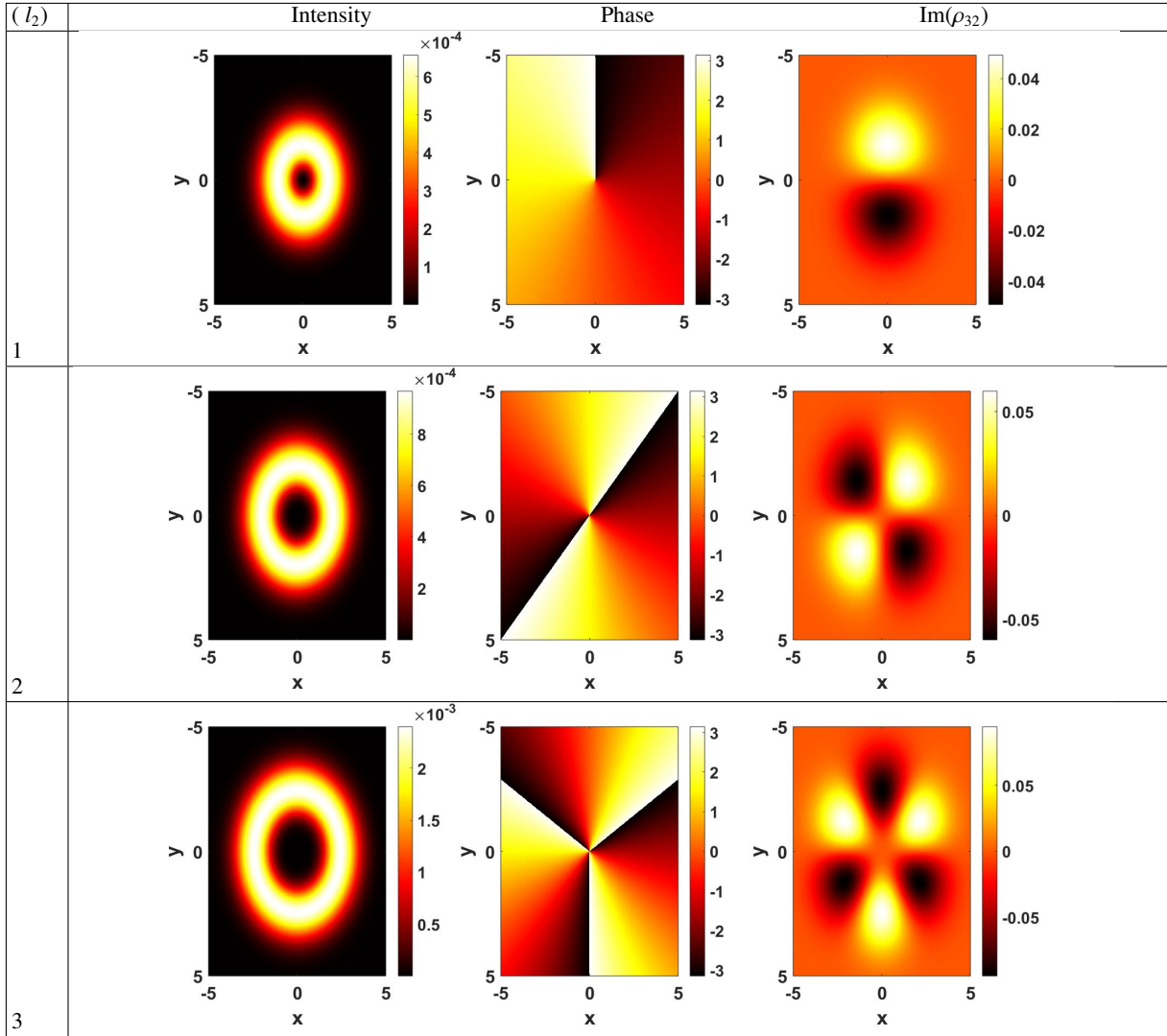


TABLE I: Intensity (first column), phase profile (second column) and, $\text{imag}(\rho_{32})$ of the generated field of rabi frequency Ω_3 for different modes of coupling LG field, i.e, $l_2 = 1, 2$ and, 3 . The parameters are $\Omega_1 = 5\gamma$, $\Omega_2 = 0.5\gamma$, and $Z = L$.

ferent values of Ω_{01} . As we increase Ω_{01} , the intensity null at $r/\omega = 0$ becomes prominent.

Additionally, in Fig.4b, we show the intensity profile of the generated Gaussian and HG beams. Alternatively, one can generate such HG beams, also by increasing the optical depth (results not shown), as mentioned in Sec. IIA.

III. MICROWAVE GENERATION WITH Λ -TYPE CONFIGURATION

Now we select the Λ -type three-level configuration of an atomic ensemble for the generation of a field in the microwave regime. The relevant energy levels $|1\rangle$, $|2\rangle$, and $|3\rangle$ are shown in Fig. 5. The transitions $|1\rangle \leftrightarrow |3\rangle$ and $|2\rangle \leftrightarrow |3\rangle$ are coupled via EM field of frequency ω_1 and ω_3 , respectively, in the visible regime. As mentioned before, in the presence of

a dc electric field, these types of systems exhibit the absence of inversion symmetry, so that the second-order susceptibility becomes non-zero. This lack of symmetry gives rise to the three-wave mixing and all three transitions becomes dipole-allowed due to the mixing of energy levels of even and odd parity. In this case, we generate a signal of frequency $\omega_2 = \omega_1 - \omega_3$ in the microwave range. The phase matching condition is also followed: $\vec{k}_2 = \vec{k}_1 - \vec{k}_3$. Ω_i is the rabi frequency of the fields, where $i = 1, 2$, and 3 .

In the context of the Λ system, there are two possibilities for choosing the coupling and the control fields. One can either choose using Ω_3 as the control field and Ω_1 as the coupling field or vice versa. In the following, we will comprehensively outline both of these configurations in sequence.

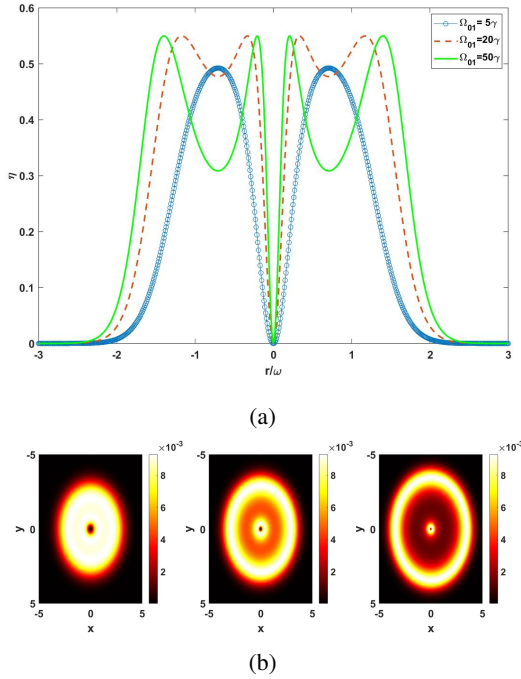


FIG. 3: (a) Variation of the η as a function of r/w when $\Omega_{01} = 5\gamma$ (blue, circled dots), 20γ (red, dash), and 50γ (green, solid); (b) intensity profile of the generated vortex beam when $\Omega_{01} = 5\gamma$, 20γ , and 50γ , respectively, and the other parameters $\Omega_2 = 0.5\gamma$, and $\omega = 2$ mm. We have chosen $l_3 = 1$ at $Z = L$.

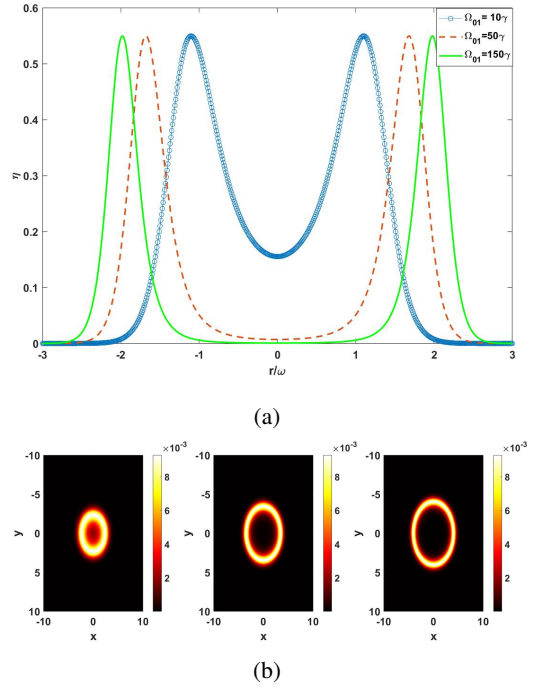


FIG. 4: a) Variation of the η as a function of r/w when $\Omega_{01} = 10\gamma$ (blue, circled dots), 50γ (red, dash), and 150γ (green, solid); (b) intensity profile of the generated vortex beam when $\Omega_{01} = 10\gamma$, 50γ , and 150γ , respectively, and the other parameters $\Omega_2 = 0.5\gamma$, and $\omega = 2$ mm. We have chosen $l_3 = 0$ at $Z = L$.

A. Ω_3 is control field and Ω_1 is coupling field

In this case, we consider $\Omega_3 \gg \Omega_1$. Since Ω_3 is the stronger field, it will not be affected by the nonlinear interaction. To find the coherence $\tilde{\rho}_{21}$ and $\tilde{\rho}_{31}$, we solve Eq. 4 up to the first order of Ω_1 , at the steady state. We assume the resonance condition, i.e., Δ_1 , Δ_2 and Δ_3 are all zero and also the decay rates γ_{13} and γ_{32} are equal to γ , while $\gamma_{12} = 2\gamma$. The relevant coherences thus take the following forms:

$$\tilde{\rho}_{21} = \frac{-i8\gamma\Omega_2 + 4\Omega_1\Omega_3^*}{16\gamma^2 + 5|\Omega_3|^2}, \quad \tilde{\rho}_{31} = \frac{-i8\gamma\Omega_1 + 4\Omega_2\Omega_3^*}{16\gamma^2 + 5|\Omega_3|^2}. \quad (10)$$

We next solve the following Maxwell's equation only for Ω_2 and Ω_1 :

$$\frac{\partial\Omega_2}{\partial z} = i\frac{\alpha_{21}\gamma_{21}}{2L}\tilde{\rho}_{21}^{(1)}, \quad \frac{\partial\Omega_1}{\partial z} = i\frac{\alpha_{31}\gamma_{32}}{2L}\tilde{\rho}_{31}^{(1)}. \quad (11)$$

For an initial condition $\Omega_2(z=0) = 0$ and $\Omega_1(z=0) = \Omega(0)$, the Rabi frequency of the generated field can be obtained as

$$\Omega_2(z) = \frac{-i\Omega_1(0)\Omega_3^*}{\sqrt{\gamma^2 - 2|\Omega_3|^2}} \left[\exp\left(\frac{2\alpha\gamma(3\gamma - \sqrt{\gamma^2 - 2|\Omega_3|^2})z}{L(16\gamma^2 + 5|\Omega_3|^2)}\right) - \exp\left(\frac{2\alpha\gamma(3\gamma + \sqrt{\gamma^2 - 2|\Omega_3|^2})z}{L(16\gamma^2 + 5|\Omega_3|^2)}\right) \right]. \quad (12)$$

1. Efficiency

As mentioned before, the generation efficiency is defined as the ratio of the intensities of the generated field and the input field. So, in this case, the efficiency η is given by:

$$\begin{aligned} \eta &= \left(\frac{|\Omega_2(z)|}{|\Omega_1(0)|} \right)^2 \\ &= \frac{|\Omega_3|^2}{\gamma^2 - 2|\Omega_3|^2} \left[\exp\left(\frac{2\alpha\gamma(3\gamma - \sqrt{\gamma^2 - 2|\Omega_3|^2})z}{L(16\gamma^2 + 5|\Omega_3|^2)}\right) - \exp\left(\frac{2\alpha\gamma(3\gamma + \sqrt{\gamma^2 - 2|\Omega_3|^2})z}{L(16\gamma^2 + 5|\Omega_3|^2)}\right) \right]^2 \end{aligned} \quad (13)$$

The term $\sqrt{\gamma^2 - 2|\Omega_3|^2}$ plays a central role in the expression for η . Given that Ω_3 represents the strong field, we consistently have $\gamma \ll \Omega_3$. Consequently, this term becomes imaginary, leading to oscillatory behavior in η (as illustrated in Fig. 6a). This oscillation extends to the intensity of the generated field within the medium.

The system exhibits an energy exchange between the generated and coupling fields, resulting in oscillations in the intensity of the generated field. By appropriately selecting the value of Z/L , we can optimize the intensity to achieve a maximum value.

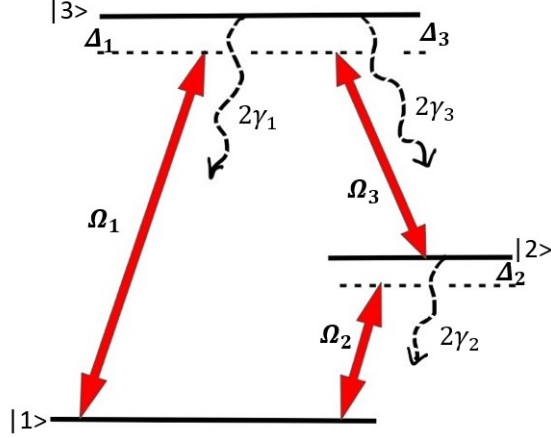


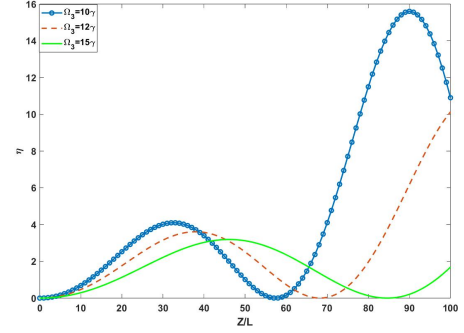
FIG. 5: Relevant energy level configuration of the Λ -type three-level atomic configuration.

2. Transfer of OAM from coupling to the Generated field

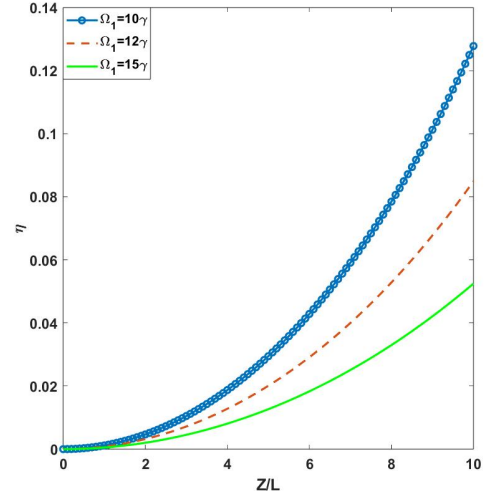
From the Eq. (12) we can see that Ω_2 is proportional to the term $\Omega_1(0)\Omega_3^*$. So the OAM of both fields Ω_1 and Ω_3 can be transferred to the generated field Ω_2 . In this section, we consider the coupling field as an LG beam. The phase singularity that is carried by the coupling field is transferred to the generated microwave field, and the field of the topological charge $l_2 = l_1$ comes out from the medium. In the first column of table II, we display the intensity profile of the generated field, which exhibits a doughnut-like pattern. In the second column, the variation of phase in transverse direction corresponding to the $l_1 = 1, 2,$ and 3 is displayed. The third column presents $\text{Im}(\rho_{21})$, where we observe $2l_1$ numbers of petals, revealing the absorption pattern of the generated field in the transverse direction.

3. Transfer of OAM from control field to Generated field

Next, we consider the control field to have an LG intensity profile. As $\Omega_2 \propto \Omega_1(0)\Omega_3^*$, one can transfer its OAM to the generated beam, which becomes an LG beam with the opposite sign of the topological charge of the control field, while its intensity pattern depends on the strength of the control field. For example, if the intensity of the control field is not strong enough, one can get only one doughnut around an intensity null. Upon the strength of the control field ($l = 1$), one ring of the generated field splits into two (see Fig. 7a). As in the case of V-type configuration, one can also construct the HGB by applying the Gaussian control field ($l = 0$) of high intensity (see Fig. 7b).



(a)



(b)

FIG. 6: Variation of η as a function of Z/L , when (a) Ω_3 is the control field for $\Omega_3 = 10\gamma$ (blue, dots), 12γ (red, dash), 15γ (green, solid) and (b) Ω_1 is the control field for $\Omega_1 = 10\gamma$ (blue, dots), 12γ (red, dash), 15γ (green, solid).

B. When Ω_1 is control field and Ω_3 is coupling field

In this case, $\Omega_1 \gg \Omega_3$. We perturbatively solve Eq. (4) in steady state up to the first order of Ω_3 and obtain the following analytical expressions for the coherences $\tilde{\rho}_{21}$ and $\tilde{\rho}_{32}$:

$$\tilde{\rho}_{21}^{(1)} = \frac{-4i\gamma\Omega_2 + 2\Omega_1\Omega_3^*}{8\gamma^2 - 3|\Omega_1|^2}, \quad \tilde{\rho}_{32}^{(1)} = \frac{-2\Omega_1\Omega_2}{8\gamma^2 - 3|\Omega_1|^2}. \quad (14)$$

For the propagation of the fields Ω_2 and Ω_3 into the medium, we solve the following Maxwell's equations:

$$\frac{\partial\Omega_2}{\partial z} = i\frac{\alpha_{21}\gamma_{21}}{2L}\tilde{\rho}_{21}^{(1)}, \quad \frac{\partial\Omega_3}{\partial z} = i\frac{\alpha_{32}\gamma_{32}}{2L}\tilde{\rho}_{32}^{(1)}. \quad (15)$$

with the initial conditions $\Omega_3(z=0) = \Omega_3(0)$ and $\Omega_2(z=0) =$

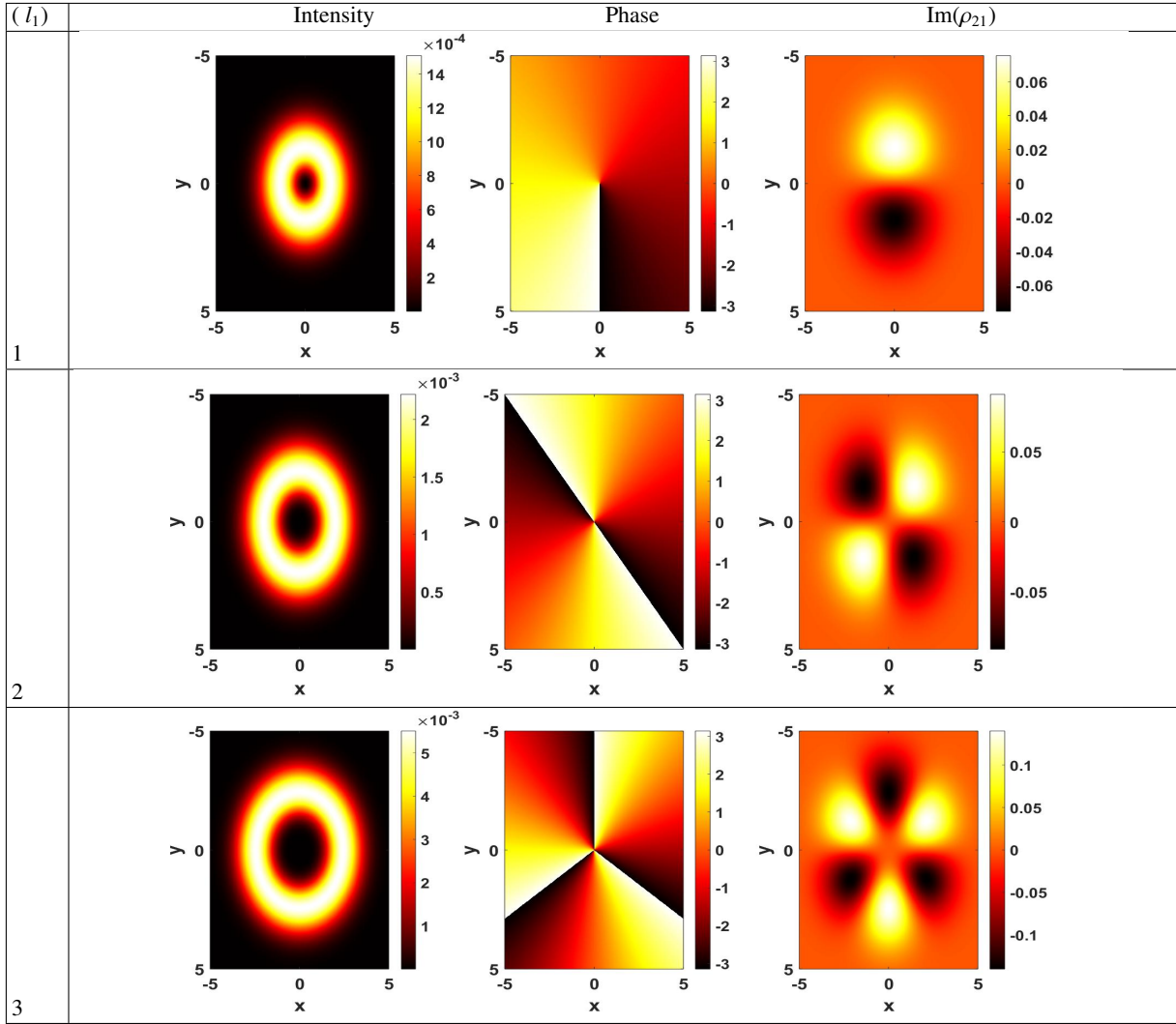


TABLE II: Intensity (first column), phase profile (second column) and, $\text{imag}(\rho_{21})$ (third column) of the generated field of the Rabi frequency Ω_2 for different modes of coupling LG field, i.e, $l_1 = 1, 2,$ and 3 . The parameters are $\Omega_3 = 5\gamma$, $\Omega_{01} = 0.5\gamma$, $w = 2$ mm, and $Z = L$.

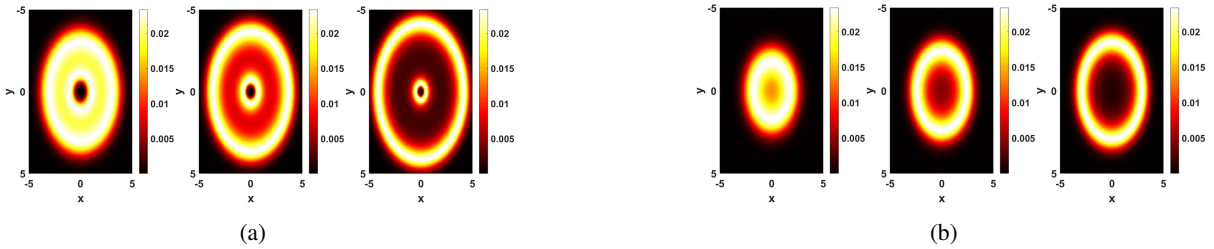


FIG. 7: Intensity profile of the generated vortex beam for $\Omega_{03} = 5\gamma, 10\gamma, 20\gamma$ respectively, (a) for $l_1=1$ and (b) for $l_1=0$. The parameters are $\Omega_1 = 0.5\gamma$, $w = 2$ mm, and $Z = L$.

0. We get the following expression for Ω_2 :

$$\Omega_2(z) = \frac{i\Omega_3^*(0)\Omega_1}{2\sqrt{\gamma^2 + 4|\Omega_1|^2}} \left[\exp\left(\frac{\alpha\gamma(\gamma - \sqrt{\gamma^2 + 4|\Omega_1|^2})z}{L(8\gamma^2 - 3|\Omega_1|^2)}\right) - \exp\left(\frac{\alpha\gamma(\gamma + \sqrt{\gamma^2 + 4|\Omega_1|^2})z}{L(8\gamma^2 - 3|\Omega_1|^2)}\right) \right] \quad (16)$$

8

1. Efficiency

The above Eq. (16) indicates that Ω_2 grows as z increases, without any oscillating or damping terms. In contrast, in the

first case, when Ω_3 is the control field, Ω_2 yields an oscillatory solution. This amplification effect is illustrated in Fig. 6b, in which we have displayed the variation of η with the normalized propagation distance, alongside the amplification of the coupling field. Since this configuration satisfies the conditions for parametric amplification, the generated field experiences significant amplification within a medium characterized by a Λ -type energy level configuration.

2. Transfer of OAM to the generated field

As stated in Eq. (16), Ω_2 varies in direct proportion to $\Omega_3^*(0)\Omega_1$. This implies that the phase singularity present in either the coupling or the control field can be transferred to the generated field, similar to our approach in the V-system and the first case of the Λ -type system.

IV. CONTROLLED-NOT GATE USING OAM STATES

The results obtained for the Λ configuration can be interpreted as a controlled-NOT (CNOT) gate in the OAM basis [32] of three fields. As we have observed, these fields satisfy the OAM conservation $l_2 = l_1 - l_3$. This means that we have $l_2 = 0$ if l_1 and l_3 are equal and l_2 is 1 if l_1 and l_3 differ by unity. Considering l_1 as the control qubit and l_2 as the target qubit, we can identify the following CNOT logic in the basis $|l_1, l_3\rangle \rightarrow |l_1, l_2\rangle$:

$$\begin{aligned} |00\rangle &\longrightarrow |00\rangle \\ |01\rangle &\longrightarrow |01\rangle \\ |10\rangle &\longrightarrow |11\rangle \\ |11\rangle &\longrightarrow |10\rangle \end{aligned}$$

In Table III, we have shown all of the above four logic operations of the CNOT in the OAM basis using Λ -configuration.

Similarly, in the V-configuration, where l_1 serves as the control qubit, the transformation $(l_1, l_2) \rightarrow (l_1, l_3)$ meets the criteria for a CNOT gate.

V. DISCUSSION

In this study, we propose a method for generating an em field in the microwave range, using the difference frequency generation process. To make the relevant transition dipole-allowed, one would need to apply a dc electric field to the atomic vapor, causing the mixing of states with even and odd parity and enabling second-order non-linearity. Here, the fine structure splittings are negligible compared to the Stark splittings whenever the magnitude of the applied electric field is in the range of 10^3 - 10^4 V/cm [24].

To illustrate our proposal of using the second harmonic generation, we provide two examples involving hydrogenic states. In the first example, the state $|2, 1, 1\rangle$ (in the $|n, l, m_l\rangle$ basis) can be identified as the ground state, while the states $\frac{1}{\sqrt{3}}(\frac{1}{\sqrt{2}}|3, 2, 0\rangle - \sqrt{\frac{3}{2}}|3, 1, 0\rangle + |3, 0, 0\rangle)$ and $\frac{1}{\sqrt{3}}(\frac{1}{\sqrt{2}}|3, 2, 0\rangle + \sqrt{\frac{3}{2}}|3, 1, 0\rangle + |3, 0, 0\rangle)$ can be chosen as the excited ones to make the V-configuration. The energy separation between the excited states is $6E_0$, where $E_0=3ea_0\epsilon$, with e representing the charge of an electron, a_0 denoting the Bohr radius, and ϵ indicating the strength of the dc electric field. For $\epsilon \sim 10^3$ V/cm, the transition between these excited states corresponds to the microwave range (with a wavelength ~ 1.30 cm), while the other transitions belong to the optical domain. One of the optical fields, carrying OAM, transfers it to the generated microwave em field.

Our second example corresponds to a Λ configuration: the ground states with an energy separation of $2E_0$ are $\frac{1}{\sqrt{2}}(|2, 0, 0\rangle - |2, 1, 0\rangle)$ and $\frac{1}{\sqrt{2}}(|2, 0, 0\rangle + |2, 1, 0\rangle)$, while the state $\frac{1}{\sqrt{2}}(|3, 2, -1\rangle + |3, 1, -1\rangle)$ can be chosen as the excited state. In this case, the microwave em field of wavelength 1.47 mm can be generated by the transition between two low-lying states, if the strength of the electric field is 10^3 V/cm.

Note that, due to the limiting value of the dc electric field, we are currently able to generate only higher-frequency microwaves. For lower-frequency microwaves, one needs to explore alternative methods.

VI. CONCLUSIONS

We have investigated how to generate a microwave field with an OAM using two different three-level configuration of atomic vapor. We also identify our result with a CNOT gate in the OAM basis. We proposed use of three-wave mixing process, in which two optical fields together create the microwave field. One can introduce a phase singularity in the microwave field, by choosing suitable OAMs in the optical fields.

In the case of Λ configuration, the efficiency of generating the microwave field can be either exponentially increasing or somewhat oscillatory with the propagation length, depending upon the choice of the transition in which the control field is applied. On the other hand, for a V-configuration, the field gets parametrically amplified as it propagates deeper into the medium. Further, by changing the strength of the Gaussian control field, the rings of the LG beam get split, leading to a HGB.

To summarize, our proposed method achieves the generation of an LG beam in the microwave regime through a series of steps involving difference frequency generation, phase singularity, and intensity manipulation. Additionally, we can utilize these LG fields of orthogonal OAM states for quantum computing and quantum information processing. Our research also holds promise for future advancements in the field of microwave communication.

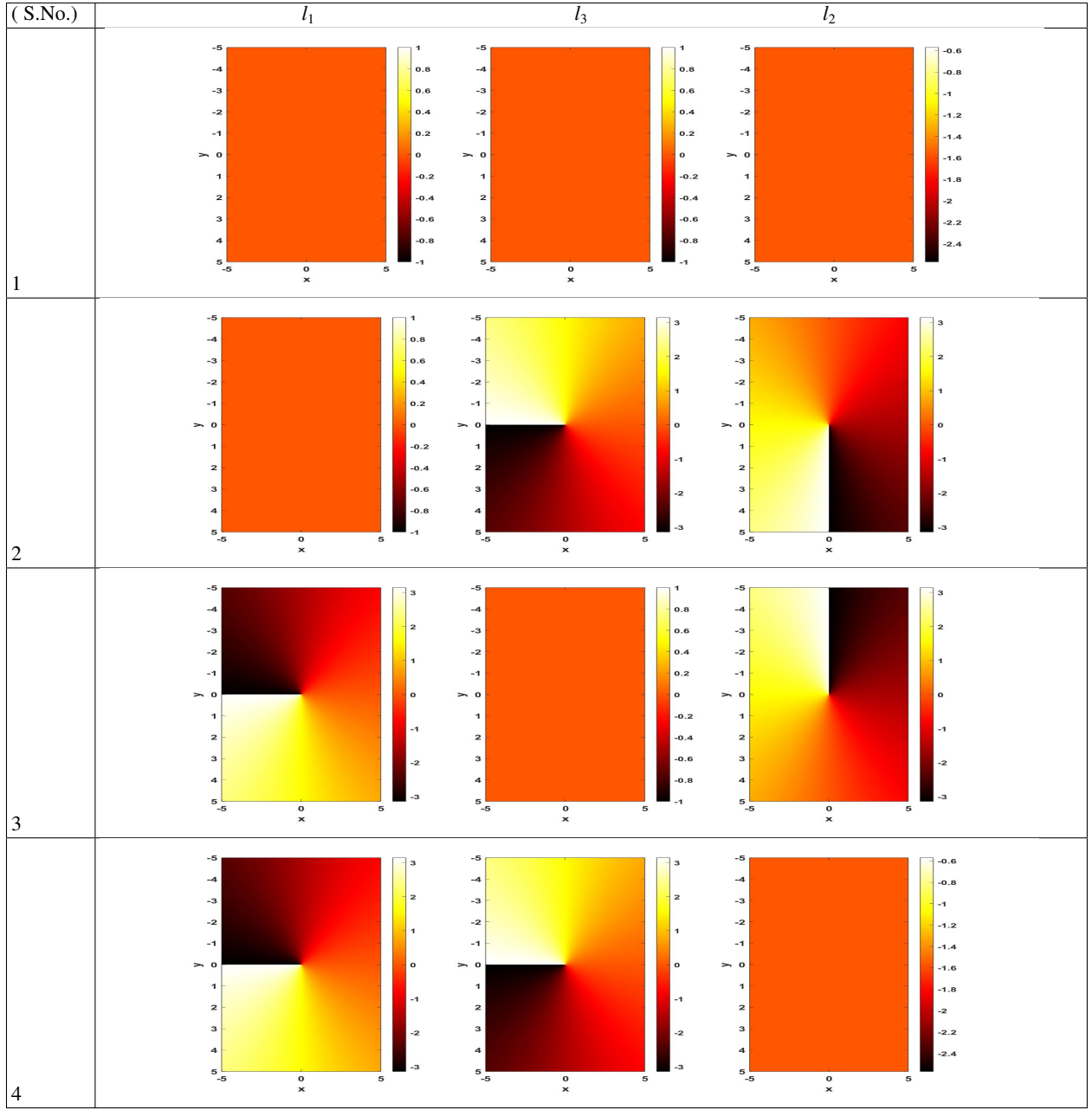


TABLE III: CNOT gate using Λ -system. The (l_1, l_3) are $(0,0)$ (first row), $(0,1)$ (second row), $(1,0)$ (third row), and $(1,1)$ (fourth row), with the corresponding outputs $l_2 = 0, 1, 1, 0$, respectively. The parameters are $\Omega_{03} = 0.5\gamma$, $\Omega_{01} = 0.5\gamma$, $w = 2$ mm, and $Z = L$.

- [1] L. Allen, M. W. Beijersbergen, R. J. C. Spreeuw, and J. P. Woerdman, *Phys. Rev. A* **45**, 8185 (1992).
- [2] L. Allen, M. Padgett, and M. Babiker (Elsevier, 1999) pp. 291–372.
- [3] M. J. Padgett and L. Allen, *Journal of Optics B: Quantum and Semiclassical Optics* **4**, S17 (2002).
- [4] N. R. Heckenberg, R. McDuff, C. P. Smith, and A. G. White, *Opt. Lett.* **17**, 221 (1992).
- [5] L. Zhu and J. Wang, *Scientific reports* **4**, 7441 (2014).
- [6] N. Matsumoto, T. Ando, T. Inoue, Y. Ohtake, N. Fukuchi, and T. Hara, *J. Opt. Soc. Am. A* **25**, 1642 (2008).
- [7] M. P. L. Allen, S.M. Barnett, CRC Press. ((2003)).
- [8] N. S. Mallick and T. N. Dey, *J. Opt. Soc. Am. B* **37**, 1857 (2020).
- [9] J. Ruseckas, V. c. v. Kudriašov, I. A. Yu, and G. Juzeliūnas, *Phys. Rev. A* **87**, 053840 (2013).

-
- [10] D.-S. Ding, Z.-Y. Zhou, B.-S. Shi, X.-B. Zou, and G.-C. Guo, *Opt. Lett.* **37**, 3270 (2012).
- [11] N. Radwell, T. W. Clark, B. Piccirillo, S. M. Barnett, and S. Franke-Arnold, *Phys. Rev. Lett.* **114**, 123603 (2015).
- [12] J. Ruseckas, A. Mekys, and G. Juzeliūnas, *Journal of Optics* **13**, 064013 (2011).
- [13] J. Ruseckas, A. Mekys, and G. Juzeliūnas, *Phys. Rev. A* **83**, 023812 (2011).
- [14] H. R. Hamed, J. Ruseckas, and G. Juzeliūnas, *Phys. Rev. A* **98**, 013840 (2018).
- [15] Z. Amini Sabegh, M. Mohammadi, M. Maleki, and M. Mahmoudi, *Journal of the Optical Society of America B* **36**, 2757 (2019).
- [16] M. M. Zahra Amini Sabegh, Mohammad Ali Maleki, *Scientific Reports* **9**, 3519 (2019).
- [17] E. Paspalakis, S.-Q. Gong, and P. L. Knight, *Optics Communications* **152**, 293 (1998).
- [18] H. R. Hamed, J. Ruseckas, E. Paspalakis, and G. Juzeliūnas, *Phys. Rev. A* **99**, 033812 (2019).
- [19] S. H. Asadpour, E. Paspalakis, and H. R. Hamed, *Phys. Rev. A* **103**, 063705 (2021).
- [20] Z. Mao, *Journal of Physics: Conference Series* **1885**, 022062 (2021).
- [21] R. A. Beth, *Phys. Rev.* **50**, 115 (1936).
- [22] Y. Y. et al., *Nature Communications* **5**, 4876 (2014).
- [23] M. Chen, L. Jiang, and W. Sha, *IEEE Transactions on Antennas and Propagation* **65**, 396 (2017), publisher Copyright: © 1963-2012 IEEE.
- [24] R. Boyd and L.-Q. Xiang, *IEEE Journal of Quantum Electronics* **18**, 1242 (1982).
- [25] R. W. Boyd, in *Nonlinear Optics (Third Edition)*, edited by R. W. Boyd (Academic Press, Burlington, 2008) third edition ed., pp. 135–206.
- [26] R. W. Boyd, in *Nonlinear Optics (Third Edition)*, edited by R. W. Boyd (Academic Press, Burlington, 2008) third edition ed., pp. 69–133.
- [27] K. Dholakia, N. B. Simpson, M. J. Padgett, and L. Allen, *Phys. Rev. A* **54**, R3742 (1996).
- [28] D. S. Bethune, R. W. Smith, and Y. R. Shen, *Phys. Rev. A* **17**, 277 (1978).
- [29] A. Flusberg, T. Mossberg, and S. R. Hartmann, *Phys. Rev. Lett.* **38**, 59 (1977).
- [30] Y. Wu and X. Yang, *Phys. Rev. A* **70**, 053818 (2004).
- [31] R. Boyd, *Nonlinear Optics*, Electronics & Electrical (Academic Press, 2003).
- [32] L. Wang, X. Zhang, A. Li, Z. Kang, H. Wang, and J. Gao, *Journal of Luminescence* **228**, 117628 (2020).